

Effects of flanking genes on the phenotypes of mice deficient in basigin/CD147[☆]

Sen Chen^a, Kenji Kadomatsu^{a,*}, Mineo Kondo^b, Yoshiro Toyama^c,
Kiyotaka Toshimori^c, Shinji Ueno^b, Yozo Miyake^b, Takashi Muramatsu^a

^a Department of Biochemistry, Nagoya University Graduate School of Medicine, Nagoya 466-8550, Japan

^b Department of Ophthalmology, Nagoya University Graduate School of Medicine, Nagoya 466-8550, Japan

^c Department of Anatomy, Chiba University Graduate School of Medicine, Chiba, Japan

Received 23 August 2004

Abstract

The induction of null mutations by means of homologous recombination is a powerful technique for clarifying the biological activities of target genes. However, the problems of the genetic background and flanking genes should be borne in mind. Here we employed a breeding strategy to compare three lines of mice deficient in the basigin (Bsg)/CD147 gene. The first line was F2 from F1 hybrid offspring of the 129/SV chimera and C57BL/6J. The second one was from a C57BL/6J congenic line. Both lines showed high embryonic lethality, sterility, and blindness. The third one was 'reverse F2' from 'reverse F1' hybrid offspring of the C57BL/6J congenic line and 129/SV. Surprisingly, this line showed a normal birth rate, while sterility and blindness persisted. Our results clearly separate the effects of the induced null mutation from those of flanking genes and the genetic background, and provide a useful means of investigating the biological functions of Bsg.

© 2004 Elsevier Inc. All rights reserved.

Keywords: Basigin; Genetic background; Knockout mice; Embryonic lethality; Sterility; Blindness

Basigin (Bsg), a transmembrane glycoprotein, belongs to the immunoglobulin superfamily with a molecular weight of 43–66 kDa depending on the glycosylation of the core protein (27 kDa) [1–3]. It was independently identified by several groups and given different names: gp 42 in the mouse [2]; OX-47 [4] and CE9 [5] in the rat; HT7 [6,7], neurothelin [8,9], and 5A11 [10] in the chicken; and M6 [11] and EMMPRIN [11] in man, which suggest the multifunctional characteristic of Bsg. Based on these data, we produced *Bsg*-deficient mice (*Bsg* ^{−/−}) and, indeed, found multiple phenotypes. *Bsg* ^{−/−} mice are rarely born due to the embryonic loss around the time

of implantation [13]. Both males and females are sterile. Impaired spermatogenesis (arrest at the metaphase of the first meiosis) is observed in *Bsg* ^{−/−} mice [13]. The female sterility is mainly due to the failure of fertilization and implantation [13,14]. Retinal degeneration leading to dysfunction is also detected in *Bsg* ^{−/−} mice [15,16]. In addition, *Bsg* ^{−/−} mice show various disorders related to neural behavior such as poor performance in learning and memory [17], decreased sensitivity to irritating odors [18], and increased sensitivity to electric foot shock [17].

Gene targeting technology to produce null mutations in mice provides a powerful tool for investigating the functions of specific gene products. However, it has been increasingly realized that targeted loci show disparate phenotypes depending on the genetic background of the mouse strains. For example, p53-deficient mice show a high susceptibility to the early development of sponta-

[☆] Abbreviations: Bsg, basigin; ERG, electroretinogram; MCT, monocarboxylate transporter.

* Corresponding author. Fax: +81 52 744 2065.

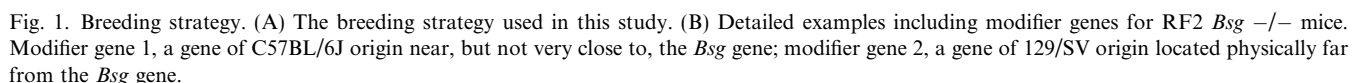
E-mail address: kkadoma@med.nagoya-u.ac.jp (K. Kadomatsu).

The high embryonic lethality observed for *Bsg* $-/-$ mice hampers detailed studies on molecular mechanisms underlying the sterility and blindness in *Bsg* deficiency. We speculated that the genetic background might have an influence on the phenotype of embryonic lethality, since this phenotype shows incomplete penetrance, while sterility and blindness occur without exception. This prompted us to employ a breeding strategy to solve the problems related to the genetic background and flanking genes.

Mice. The procedure for targeting of the *Bsg* gene was that described previously [13]. The ES cells used were D3 derived from 129/SV. The breeding strategy is summarized in Fig. 1A. The first line of *Bsg*^{−/−} mice was generated as described previously [13]. Thus, the 129/SV chimera and C57BL/6J were mated to produce F1 hybrid offspring. F2 for analysis was then generated by intercrossing F1 siblings. The second one was generated from a C57BL/6J congenic line that was backcrossed 13 times. The third one was ‘reverse F2 (RF2)’ generated by intercrossing ‘reverse F1 (RF1)’ hybrid offspring of the C57BL/6J congenic line and 129/SV [25]. Care of the mice was performed in accordance with Nagoya University Animal Institute Guidelines. Genotyping was performed by PCR as described previously [13].

Electroretinographic recordings. Mice were dark-adapted overnight, and then anesthetized with an intramuscular injection of 86 mg/kg ketamine and 13 mg/kg xylazine. The pupils were dilated with topical 0.5% tropicamide and 0.5% phenylephrine HCL, and then the mice were placed on a heating pad. ERGs were recorded with a gold-wire loop electrode placed on the cornea.

The mice were placed in a Ganzfeld bowl and stimulated with stroboscopic stimuli of 1.0 log cd-s/m² (photopic units) maximum intensity. Neutral density filters were used to reduce the stimulus intensity. Seven steps of stimulus intensities ranging from -6.2 to 1.0 log cd-s/m² were used for the scotopic electroretinographic (ERG) recordings, and four steps of stimuli ranging from -0.8 to



1.0 log cd-s/m² for the photopic ERG recordings. The photopic ERGs were recorded on a rod-suppressing white background of 1.3 log cd/m².

Results

Increased birth rate and viability of RF2 *Bsg* $-/-$ mice

Among F2 derived from F1 hybrid offspring of the 129/SV chimera and C57BL/6J (called 'F2' in this paper), *Bsg* $-/-$ mice that were born and survived for 2 months after birth accounted for only 5.9% and 3.5% of the offspring, respectively [13]. We produced additional two lines of *Bsg* $-/-$ mice: one was generated through intercrossing a C57BL/6J congenic line with 13 backcrosses (called 'congenic'), and the other one

was RF2 derived from RF1 hybrid offspring of the C57BL/6J congenic line and 129/SV (called 'RF2') (Fig. 1). The congenic *Bsg* $-/-$ mice exhibited a similar phenotype to that of F2 *Bsg* $-/-$ mice, the birth rate being 7.0% (Table 1). By contrast, RF2 *Bsg* $-/-$ mice showed a dramatically improved birth rate (21.7%). The congenic *Bsg* $-/-$ mice showed decreased survival after birth like F2 *Bsg* $-/-$ mice, while the postnatal viability of RF2 *Bsg* $-/-$ mice was significantly increased (Table 1, Figs. 1A and B).

Next we compared the growth of the surviving mice. Both congenic and RF2 *Bsg* $-/-$ mice could survive if they did not die within 1 month after birth (Figs. 2A and B). RF2 siblings grew well regardless of the genotype (Fig. 2C), whereas congenic *Bsg* $-/-$ mice were smaller in size than *Bsg* $+/+$ and $+/-$ siblings (Fig. 2D), like in the case of F2 *Bsg* $-/-$ mice [13]. We could not evaluate statistically the differences among the congenic siblings since we could obtain only 3 *Bsg* $-/-$ mice from this strain. Figs. 2C and D show growth curves for only male mice, female mice showing similar curves (data not shown).

RF2 *Bsg* $-/-$ mice are sterile

Both sexes of F2 *Bsg* $-/-$ mice are infertile [12]. We investigated the reproduction of RF2 *Bsg* $-/-$ mice (Table 2). Although wild \times wild pairs were impregnated immediately after mating, male wild \times female *Bsg* $-/-$, male *Bsg* $-/-$ \times female wild, and male *Bsg* $-/-$ \times female *Bsg* $-/-$ pairs could not be impregnated until 3 months.

Table 1
Numbers of newborn and adult mice (2-month-old) from heterozygous parents

	<i>Bsg</i> $+/+$	<i>Bsg</i> $+/-$	<i>Bsg</i> $-/-$	Total
Newborn				
RF2	30 (23.3) ^a	71 (55.0)	28 (21.7) [*]	129
Congenic	48 (33.6)	85 (59.4)	10 (7.0)	143
Adult mice				
RF2	30 (23.3)	71 (55.0)	19 (14.7) ^{**}	120
Congenic	43 (30.1)	79 (55.2)	3 (2.1)	125

^a % against the total number of newborn is shown in parentheses.

^{*} $p < 0.005$ vs. congenic *Bsg* $-/-$ (χ^2 test).

^{**} $p < 0.005$ vs. congenic *Bsg* $-/-$ (χ^2 test).

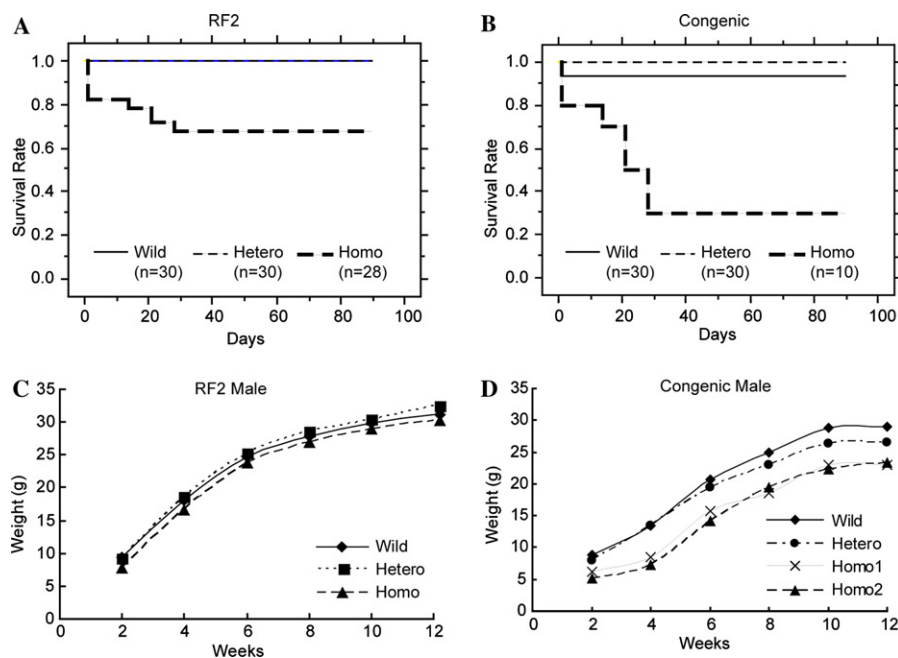


Fig. 2. Improved survival rate in RF2 *Bsg* $-/-$ mice. (A) The survival curve for RF2 mice. *Bsg* $+/+$ (Wild): $n = 28$; *Bsg* $+/-$ (Hetero): $n = 37$; and *Bsg* $-/-$ (Homo): $n = 28$. The curves for *Bsg* $+/+$ and *Bsg* $+/-$ are the same. (B) The survival curve for C57BL/6J congenic mice. *Bsg* $+/+$ (Wild): $n = 30$; and *Bsg* $+/-$ (Hetero): $n = 30$; *Bsg* $-/-$ (Homo): $n = 10$. (C) The growth curve for male RF2 mice. (D) The growth curve for female RF2 mice.

Table 2
Reproduction of RF2 mice

Male	Female	Newborn
+/+ (5) ^a	-/- (5)	-
-/- (5)	+/+ (5)	-
-/- (5)	-/- (3)	-
+/+ (5)	+/+ (5)	+ ^b

^a The numbers in parentheses indicate the numbers of animals used.
^b Every pair produced several pups and showed normal reproduction.

The congenic *Bsg* $-/-$ mice were also infertile (data not shown). As shown in Fig. 3, most of the spermatocytes in the RF2 *Bsg* $-/-$ mice were arrested and degenerated at the metaphase of the first meiosis, which is the same as that reported for F2 *Bsg* $-/-$ [13].

RF2 Bsg -/- mice show retinal dysfunction

Bsg $-/-$ mice derived from the C57BL/6J congenic line (5–7th generation) from 5 to 41 weeks of age exhibit progressive decreases in the amplitudes of all components of both photopic and scotopic electroretinograms (ERGs) [15]. Consistently, the photoreceptor cells degenerate gradually and are almost completely ablated by 41 weeks [15]. Therefore, we examined the histology of the retina of RF2 siblings. As shown in Fig. 4, the retina of RF2 *Bsg* $-/-$ mice exhibited severe degeneration, the degeneration being most prominent in the cone and rod photoreceptor layer. At 30-weeks-of-age, the length of the outer segment of the photoreceptor was reduced in the *Bsg* $-/-$ mice to 15% of the length in *Bsg* $+/+$ mice and the nuclei in the outer nuclear layer were reduced to approximately 35% of the number in *Bsg* $+/+$ mice (Fig. 4). The thickness and cell numbers in the inner retina in the *Bsg* $-/-$ mice remained unchanged.

To evaluate the retinal function in vivo, ERGs were recorded for RF2 *Bsg* $+/+$ and $-/-$ mice. Representa-

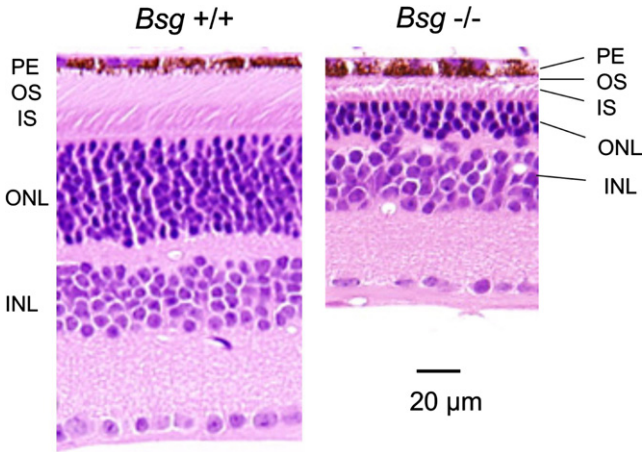


Fig. 4. Retinal histology at the posterior pole in *Bsg* $+/+$ and *Bsg* $-/-$ mice at 30-weeks-of-age. Compared with the *Bsg* $+/+$ mouse, the outer segments (OS) are shorter and the number of nuclei in the outer nuclear layer (ONL) is markedly reduced in the *Bsg* $-/-$ mouse. PE, retinal pigment epithelium; OS, outer segment; IS, inner segment; ONL, outer nuclear layer; and INL, inner nuclear layer.

tive dark-adapted ERGs for a *Bsg* $+/+$ and a *Bsg* $-/-$ mice of 30-weeks-of-age are shown in Fig. 5A. The ERG amplitudes were severely attenuated in *Bsg* $-/-$ mice, while those in *Bsg* $+/+$ mice remained unchanged. In the *Bsg* $-/-$ mice, the amplitude of the a-wave, which reflects the activity of rod photoreceptors, was reduced to 10% of that in the *Bsg* $+/+$ mice, and the amplitude of the b-wave, which originates from the rod bipolar cells, was reduced to 22% of that in the *Bsg* $+/+$ mice (Fig. 5B).

Light-adapted ERGs were also recorded for both types of mice, and they were severely attenuated in the *Bsg* $-/-$ mice (Fig. 5C). The amplitude of the light-adapted ERG b-wave was reduced to 30% of that in the *Bsg* $+/+$ mice (Fig. 5D).

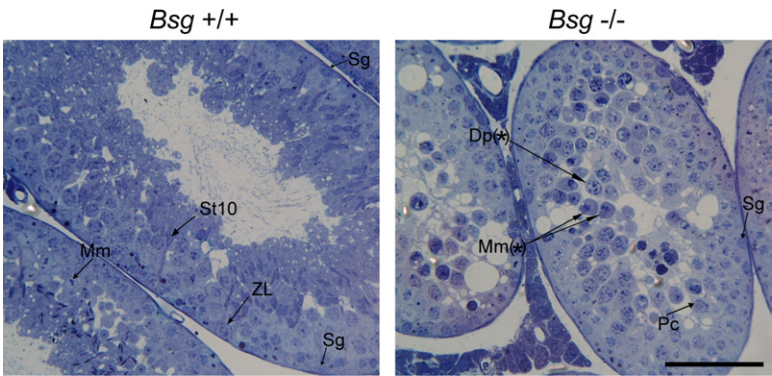


Fig. 3. Arrest of spermatogenesis in RF2 *Bsg* $-/-$ mice. Thirty-week-old RF2 *Bsg* $+/+$ and $-/-$ mice were examined. Most of the spermatocytes in the RF2 *Bsg* $-/-$ mouse were arrested and degenerated at the metaphase of the first meiosis. Dp (*), diplotene (degenerated); Mm, meiotic metaphase; Mm (*), meiotic metaphase (degenerated); Pc, pachytene spermatocyte; Sg, spermatogonium (type A); St 10, step 10 spermatid; and ZL, zygotene/leptotene spermatocyte. Bar, 100 μ m.

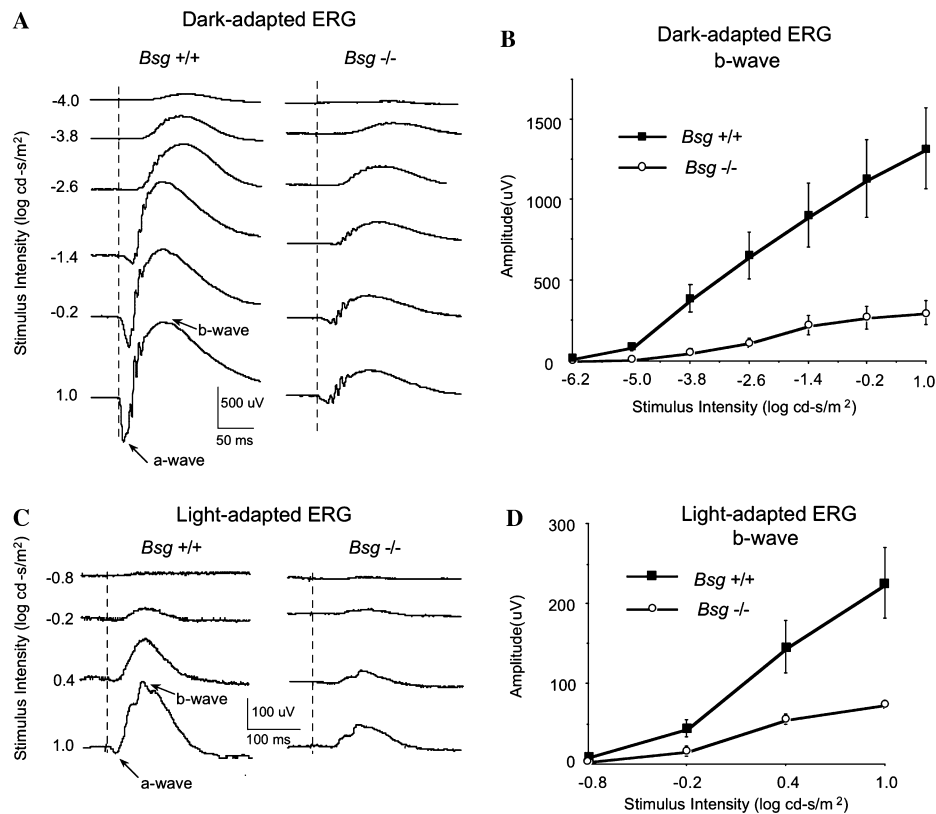


Fig. 5. Electrophoretograms recorded for 30-week-old *Bsg* $+/+$ and *Bsg* $-/-$ mice. (A) Dark-adapted ERGs elicited with six different stimulus intensities are shown. The vertical dotted lines show the onset of the stimulus. (B) Intensity–response function of the dark-adapted ERG b-wave for *Bsg* $+/+$ and *Bsg* $-/-$ mice. The means \pm SE of the means for four *Bsg* $+/+$ and four *Bsg* $-/-$ mice are shown. (C) Light-adapted ERGs elicited with four different stimulus intensities. (D) Intensity–response function of the light-adapted ERG b-wave for *Bsg* $+/+$ and *Bsg* $-/-$ mice. The means \pm SE of the means for four *Bsg* $+/+$ and four *Bsg* $-/-$ mice are shown.

These retinal studies clearly showed that there was severe degeneration in the retina of RF2 *Bsg* $-/-$ mice for both the rod and cone systems, and this degeneration was most prominent in the photoreceptor cells.

Discussion

The present study revealed that the phenotypes of *Bsg* $-/-$ mice can be divided into two categories. One comprises embryonic lethality, which is influenced by the genetic background and flanking genes. The other one includes sterility and retinal dysfunction, which are merely due to induced null mutation of the *Bsg* gene.

Regarding the action mechanism of *Bsg* explaining the retinal dysfunction in *Bsg* $-/-$ mice, the biosynthesis and translocation of monocarboxylate transporters (MCTs) are important. Lactate is known to be used as energy source by neuronal cells and is transported by MCTs [26]. Proper localization of MCTs to the cell surface is mediated by *Bsg* [26]. Consistently, the marked reduction of MCTs is observed in the pigment epithelium and neural retina of *Bsg* $-/-$ mice [27]. Thus, the

progressive retinal degeneration and dysfunction could be caused by a defect of the organized energy metabolism in *Bsg* $-/-$ mice. As it is known that MCT1 is strongly expressed in spermatocytes [28], where *Bsg* is expressed [13], it is conceivable that the physical, functional association of *Bsg* and MCT also plays a critical role in spermatogenesis.

As illustrated in Fig. 1A, the only difference between F2 and RF2 *Bsg* $-/-$ mice is in the composition of the flanking region of the *Bsg* gene, while the difference between the congenic and RF2 *Bsg* $-/-$ mice is in the composition of physically unrelated genes, which are far from the *Bsg* gene. Taken together, our data suggest that interaction between at least two modifier genes is essential for normal embryonic development of RF2 *Bsg* $-/-$ mice. The genes comprise one of C57BL/6J origin near, but not very close to, the *Bsg* gene, and one of 129/SV origin located physically far from the *Bsg* gene (Fig. 1B). RF2 *Bsg* $-/-$ mice are expected to carry the former and latter genes at probabilities of 100% and 75%, respectively (Fig. 1B). Therefore, the probability of live birth of RF2 *Bsg* $-/-$ mice is approximately 20% ($\approx 25\% \times 75\%$), which is consistent with our data (21.7%) (Table 1).

With regard to candidates for such modifiers, embigin (Emb) and integrins could be postulated. Emb, Bsg, and neuroligin comprise a subfamily of the immunoglobulin superfamily [3]. Among them, Emb is restrictively expressed during embryogenesis and involved in cell-substratum adhesion in an integrin-dependent manner [29]. Integrin is known to be physically associated with Bsg [30] and to be involved in implantation [31]. It might be possible that Emb and/or integrin play a compensatory role in implantation in *Bsg*^{−/−} mice. Efforts are needed to examine such an intriguing possibility. It has been reported that the embryonic lethal phenotypes of null mutant mice as to *Msh2-Trp53* [32], EGFR [33], and retinoblastoma-related p130 gene [34] are strain-dependent, suggesting the existence of modifier loci, although their location remains unclear. The present results suggest that at least one of the modifier genes is located near the *Bsg* gene. Our data may provide a clue for identifying a modifier gene regarding embryonic lethality.

Although *Bsg*^{−/−} mice exhibit many other important phenotypes, including many dysfunctional phenotypes related to neural or behavioral processes [13,18], they remain to be studied because of the limited number of *Bsg*^{−/−} mice so far. In our study, the birth rate and viability of *Bsg*^{−/−} mice were markedly improved, which will provide a precious tool for the investigation on the biological functions of Bsg.

Acknowledgments

We thank Satoshi Yamamoto for backcrossing *Bsg*^{+/-} to C57BL/6J. This work was supported by Grants-in-Aid for Scientific Research from the Ministry of Education, Science, Sports, Culture and Technology, Japan (14082202).

References

- [1] T. Miyauchi, T. Kanekura, A. Yamaoka, M. Ozawa, S. Miyazawa, T. Muramatsu, Basigin, a new, broadly distributed member of the immunoglobulin superfamily, has strong homology with both the immunoglobulin V domain and the β -chain of major histocompatibility complex class II antigen, *J. Biochem.* 107 (1990) 316–323.
- [2] F. Altruda, P. Cervella, M.L. Gaeta, A. Daniele, F. Giancotti, G. Tarone, G. Stefanuto, L. Silengo, Cloning of cDNA for a novel mouse membrane glycoprotein (gp42): shared identity to histocompatibility antigens, immunoglobulins and neural-cell adhesion molecules, *Gene* 85 (1989) 445–451.
- [3] T. Muramatsu, T. Miyauchi, Basigin (CD147): a multifunctional transmembrane protein involved in reproduction, neural function, inflammation and tumor invasion, *Histol. Histopathol.* 18 (2003) 981–987.
- [4] S. Fossum, S. Mallett, A.N. Barclay, The MRC OX-47 antigen is a member of the immunoglobulin superfamily with an unusual transmembrane sequence, *Eur. J. Immunol.* 21 (1991) 671–679.
- [5] C.L. Nehme, M.M. Cesario, D.G. Myles, D.E. Koppel, J.R. Bartles, Breaching the diffusion barrier that compartmentalizes transmembrane glycoprotein CE9 to the posterior-tail plasma membrane domain of the rat spermatozoon, *J. Cell Biol.* 120 (1993) 687–694.
- [6] H. Seulberger, F. Lottspeich, W. Risau, The inducible blood–brain barrier specific molecule HT7 is a novel immunoglobulin-like cell surface glycoprotein, *EMBO J.* 9 (1990) 2151–2158.
- [7] H. Seulberger, C.M. Unger, W. Risau, HT7, neurothelin, basigin, gp42 and OX-47—Many names for one developmentally regulated immunoglobulin-like surface glycoprotein on blood-brain barrier endothelium, epithelial tissue barriers and neurons, *Neurosci. Lett.* 140 (1992) 93–97.
- [8] B. Schlosshauer, K.H. Herzog, Neurothelin: an inducible cell surface glycoprotein of blood–brain barrier-specific endothelial cells and distinct neurons, *J. Cell Biol.* 110 (1990) 1261–1274.
- [9] B. Schlosshauer, Neurothelin: molecular characteristics and developmental regulation in the chick CNS, *Development* 113 (1991) 129–140.
- [10] J.M. Fadool, P.J. Linser, 5A11 antigen is a cell recognition molecule which is involved in neuronal–glial interactions in avian neural retina, *Dev. Dyn.* 196 (1993) 252–262.
- [11] W. Kasinrerker, E. Fiebigler, I. Stefanová, T. Baumruker, W. Knapp, H. Stockinger, Human leukocyte activation antigen M6, a member of the Ig superfamily, is the species homologue of rat OX-47, mouse basigin, and chicken HT7 molecule, *J. Immunol.* 149 (1992) 847–854.
- [12] C. Biswas, Y. Zhang, R. DeCastro, H. Guo, T. Nakamura, H. Kataoka, K. Nabeshima, The human tumor cell-derived collagenase stimulatory factor (renamed EMMPRIN) is a member of the immunoglobulin superfamily, *Cancer Res.* 55 (1995) 434–439.
- [13] T. Igakura, K. Kadomatsu, T. Kaname, H. Muramatsu, Q.W. Fan, T. Miyauchi, Y. Toyama, N. Kuno, S. Yuasa, M. Takahashi, T. Senda, O. Taguchi, K. Yamamura, K. Arimura, T. Muramatsu, A null mutation in basigin, an immunoglobulin superfamily member, indicates its important roles in perimplantation development and spermatogenesis, *Dev. Biol.* 194 (1998) 152–165.
- [14] N. Kuno, K. Kadomatsu, Q.W. Fan, M. Hagihara, T. Senda, S. Mizutani, T. Muramatsu, Female sterility in mice lacking the basigin gene, which encodes a transmembrane glycoprotein belonging to the immunoglobulin superfamily, *FEBS Lett.* 425 (1998) 191–194.
- [15] K. Hori, N. Katayama, S. Kachi, M. Kondo, K. Kadomatsu, J. Usukura, T. Muramatsu, S. Mori, Y. Miyake, Retinal dysfunction in basigin deficiency, *Invest. Ophthalmol. Vis. Sci.* 41 (2000) 3128–3133.
- [16] J.D. Ochieter, T.M. Moroz, K. Kadomatsu, T. Muramatsu, P.J. Linser, Retinal degeneration following failed photoreceptor maturation in 5A11/basigin null mice, *Exp. Eye Res.* 72 (2001) 467–477.
- [17] K. Naruhashi, K. Kadomatsu, T. Igakura, Q.W. Fan, N. Kuno, H. Muramatsu, T. Miyauchi, T. Hasegawa, A. Itoh, T. Muramatsu, T. Nabeshima, Abnormalities of sensory and memory functions in mice lacking Bsg gene, *Biochem. Biophys. Res. Commun.* 236 (1997) 733–737.
- [18] T. Igakura, K. Kadomatsu, O. Taguchi, H. Muramatsu, T. Kaname, T. Miyauchi, K. Yamamura, K. Arimura, T. Muramatsu, Roles of basigin, a member of the immunoglobulin superfamily, in behavior as to an irritating odor, lymphocyte response, and blood–brain barrier, *Biochem. Biophys. Res. Commun.* 224 (1996) 33–36.
- [19] L.A. Donehower, M. Harvey, H. Vogel, M.J. McArthur, C.A. Montgomery Jr., S.H. Park, T. Thompson, R.J. Ford, A. Bradley, Effects of genetic background on tumorigenesis in p53-deficient mice, *Mol. Carcinog.* 14 (1995) 16–22.

- [20] M. Harvey, M.J. McArthur, C.A. Montgomery Jr., A. Bradley, L.A. Donehower, Genetic background alters the spectrum of tumors that develop in p53-deficient mice, *FASEB J.* 7 (1993) 938–943.
- [21] D.J. Van Meyel, O.H. Sanchez-Sweetman, N. Kerkvliet, L. Stitt, D.A. Ramsay, R. Khokha, A.F. Chambers, J.G. Cairncross, Genetic background influences timing, morphology and dissemination of lymphomas in p53-deficient mice, *Int. J. Oncol.* 13 (1998) 917–922.
- [22] C.D. Sigmund, Viewpoint: are studies in genetically altered mice out of control?, *Thromb. Vasc. Biol.* 20 (2000) 1425–1429.
- [23] A. Banbury, Conference on genetic background in mice, mutant mice and neuroscience: recommendations concerning genetic background, *Neuron* 19 (1997) 755–759.
- [24] R. Gerlai, Gene-targeting studies of mammalian behavior: is it the mutation or the background genotype? *Trends Neurosci.* 19 (1996) 177, Erratum in: *Trends Neurosci.* 19 (1996) 271.
- [25] D.P. Wolfer, W.E. Crusio, H.P. Lipp, Knockout mice: simple solutions to the problems of genetic background and flanking genes, *Trends Neurosci.* 25 (2002) 336–340.
- [26] P. Kirk, M.C. Wilson, C. Heddle, M.H. Brown, A.N. Barclay, A.P. Halestrap, CD147 is tightly associated with lactate transporters MCT1 and MCT4 and facilitates their cell surface expression, *EMBO J.* 19 (2000) 3896–3904.
- [27] N.J. Philp, J.D. Ochriotor, C. Rudoy, T. Muramatsu, P.J. Linser, Loss of MCT1, MCT3, and MCT4 expression in the retinal pigment epithelium and neural retina of the 5A11/basigin-null mouse, *Invest. Ophthalmol. Vis. Sci.* 44 (2003) 1305–1311.
- [28] I. Goddard, A. Florin, C. Mauduit, E. Tabone, P. Contard, R. Bars, F. Chuzel, M. Benahmed, Alteration of lactate production and transport in the adult rat testis exposed in utero to flutamide, *Mol. Cell. Endocrinol.* 206 (2003) 137–146.
- [29] R.P. Huang, M. Ozawa, K. Kadomatsu, T. Muramatsu, Embigin, a member of the immunoglobulin superfamily expressed in embryonic cells, enhances cell-substratum adhesion, *Dev. Biol.* 155 (1993) 307–314.
- [30] F. Berditchevski, S. Chang, J. Bodorova, M.E. Hemler, Generation of monoclonal antibodies to integrin-associated proteins. Evidence that alpha3beta1 complexes with EMMPRIN/basigin/OX47/M6, *J. Biol. Chem.* 272 (1997) 29174–29180.
- [31] K.V. Reddy, S.S. Mangale, Integrin receptors: the dynamic modulators of endometrial function, *Tissue Cell* 35 (2003) 260–273.
- [32] A. Cranston, R. Fishel, Female embryonic lethality in Msh2-Trp53 nullizygous mice is strain dependent, *Mamm. Genome* 10 (1999) 1020–1022.
- [33] D.W. Threadgill, A.A. Dlugosz, L.A. Hansen, T. Tennenbaum, U. Lichti, D. Yee, C. LaMantia, T. Mourtou, K. Herrup, R.C. Harris, et al., Targeted disruption of mouse EGF receptor: effect of genetic background on mutant phenotype, *Science* 269 (1995) 230–234.
- [34] J.E. LeCouter, B. Kablar, P.F. Whyte, C. Ying, M.A. Rudnicki, Strain-dependent embryonic lethality in mice lacking the retinoblastoma-related p130 gene, *Development* 125 (1998) 4669–4679.